Temperature influence on the performance of P3HT:ICBA polymer solar cells

Ali R. Khalf, Jovana P. Gojanović, Nataša A. Ćirović, Petar S. Matavulj, *Member, IEEE*, Grant Ledet, Mark Hidalgo and Sandra Živanović, *Member, IEEE*

Abstract—Temperature (*T*) dependent performance of polymer solar cells (PSCs) with a poly (3-hexylthiophene): indene-C_{60} bisadduct (P3HT:ICBA) active layer were investigated. The current-voltage *(I-V)* characteristics of devices with two different active layer thicknesses (ALTs) were measured within a temperature range of 20 °C-65 °C. The recorded *I-V* curves showed the S-shape deviation. The *I-V* curves were also simulated by a standard drift-diffusion model that includes the influence of the surface recombination on both electrode contacts. The Arrhenius-type temperature-dependent hole mobility was introduced to reproduce the experimentally observed temperature-dependent PSC behavior. The measured power conversion efficiency (PCE) and short-circuit current *(Isc)* changed non-monotonically with *T* whereby detailed temperature trends differed for solar cells of different ALTs. The noticed effects were not present in theoretically predicted PCE and *Isc*. To match the simulated and experimental *I-V* characteristics the PCS internal quantum efficiency (IQE) was varied with *T*. We suggest that the obtained nonmonotonic IQE(*T*) dependence originates from changes in morphology caused by the influence of temperature and strongly correlates to the P3HT:ICBA thin-film thickness.

Index Terms—P3HT; solar cells; simulation; temperature.

I. INTRODUCTION

POLYMER-based bulk-heterojunction solar cells (PSCs) are an emerging renewable energy technology that enables easy, low-cost and low-environmental impact production and yields lightweight, flexible devices with the possibility of visible transparency, and large surface area. Power conversion efficiency (PCE) of PSCs has drastically improved during the last decade, surpassing 18% for single-junction cells [1], and 18.6% for tandem cells [2]. Enhancement of PCE has been accomplished through several different developmental directions. A crucial issue regarding polymer-based solar cells is how to manage the energy levels of the donor/acceptor (D/A) blends to maximize short-circuit current (*Isc*) and open-circuit voltage (*Voc*) at the same time without sacrificing the efficient charge separation [3, 4]. New donor [3, 4] and acceptor [5] materials were synthesized to accomplish this goal. Optimization of process parameters [6], annealing [7], aggregation, and morphology control [8] were used to improve the charge transport in PSCs. Much better extraction of charge carriers was accomplished by

A. R. Khalf, J. P. Gojanović, N. A. Ćirović, and P. S. Matavulj are with the School of Electrical Engineering, University of Belgrade, Belgrade 11120, Serbia (e-mail: alirkhalf@yahoo.com; jovana@etf.bg.ac.rs; natasa@etf.bg.ac.rs; matavulj@etf.bg.ac.rs).

G. Ledet, M. Hidalgo and S. Živanović are with Institute for Micromanufacturing, Louisiana Tech University, Ruston, LA 71272 USA (e-mail: grantledet@gmail.com, mkhidalgo@charter.net, sz@latech.edu).

introducing the hole and electron buffer layers [9]. Optical manipulation of light has become an increasingly popular strategy to capture solar radiation more effectively into an ultrathin photoactive layer of PSC thus to enhance the light-harvesting efficiency [10, 11].

In the meantime, a lot of theoretical research has been done resulting in the first PSC drift-diffusion model (DDM) developed by Koster et al. in 2005 [12]. A long time ago, it was established that interferential effects play a significant role in organic thin-film photovoltaic devices [13]. Therefore, an optical model based on transfer matrix formalism was soon coupled to drift-diffusion calculations, completing the image of important physical processes in PSC [13]. This model including different modifications and updates is successfully used to simulate the performance of PSC with various structures and D/A material combinations. It is also a powerful tool for the investigation of physical phenomena that undergo PSC operation [14, 15] as well as for device optimization [16]. Besides the drift-diffusion approach, some equivalent circuit models have also been proposed [17]. These models introduce the other point of view, and they account for additional electrical PSC features not included in the DDM such as parasitic resistivities and other parasitic effects. Another field that the DDM does not cover in a sufficiently detailed way is the impact of morphology and nanoscale physical processes on the efficiency of PSC. Through Monte Carlo and multiscale simulations [18], one can approach the nanostructure of the active layer and follow the excitonic and charge carrier pathways. This can lead to some crucial conclusions and hints for the fabrication of highly efficient PSC.

Summarizing the state of the art in the field of PSCs, it becomes clear that there is a lot of room for additional research by physicists, chemists, and technologists to improve PSC efficiency towards their commercialization.

It is well known that temperature and light intensity dependence of optoelectronic device performance gives a good insight into the physical processes underlying its operation. Such measurements were carried out on the PSCs to study the photogeneration and transport of charge carriers [19, 14, 15, 20 21] as well as the mechanisms of their recombination [22, 23, 24, 20]. According to our knowledge only a few papers in the literature have been dedicated to the investigation of PSC *I-V* curve temperature-dependence and consequently *Isc*, *Voc*, fill factor (FF), and PCE temperature dependences [25, 26, 27, 28, 29, 30, 20]. Among these papers just one presents the DDM model that includes the PCS temperature dependent behavior, unfortunately, without matching the model results to any experimental data [20]. Knowing the influence of the temperature on PCS performance is very important to predict the operation of the device in standard working conditions as well as for further progress in PCE optimization. To prevent unnecessary

expenses, a useful model is needed to simulate temperature-dependence of PSC.

In this paper ITO(indium tin oxide)/PEDOT:PSS (poly(3,4-hylenedioxythiophene):poly(styrenesulfonate))/P3HT:ICBA (poly(3-hexylthiophene):indene-C_{60} bisadduct)/Al solar cells with two different thicknesses of P3HT:ICBA active layer were fabricated and tested in the 20 °C to 65 °C temperature range. The S-shaped I-V characteristics were recorded under solar simulator light from which I_{sc} and PCE dependences on T were determined for each device. The device performance was simulated by the standard drift-diffusion model (DDM) that accounts for surface recombination on electrodes. The Arrhenius-type temperature-dependent hole mobility was applied [15]. It was found that the experimental PCE and I_{sc} vary non-monotonicaly with temperature (T). Also, temperature caused variation of PCE and I_{sc} for two devices with different active layer thicknesses (ALTs) was different. The DDM calculated solar cell parameters did not show such behavior. To match the simulated and measured I-V curves it was necessary to introduce the temperature-dependent internal quantum efficiency (IQE) of PSCs. The surface recombination was also taken to be temperature-dependent. The nonmonotonic change of IQE with T obtained in this way was attributed to the change of P3HT:ICBA film morphology which is, on the other hand, correlated to the active layer film thickness [31].

II. EXPERIMENT

PSC devices with glass/ ITO/ PEDOT: PSS/ P3HT:ICBA/ Al device structure were fabricated and tested at Institute for Micromanufacturing, Louisiana Tech University.

P3HT and ICBA from Sigma Aldrich with 1:0.78 wt. ratio were mixed with chlorobenzene separately and kept on a hot plate with a magnetic stirrer at 50 °C overnight. PEDOT:PSS HTL Solar Heraeus Clevios water solution from Ossila was spin-coated at 3500 RPM to deposit about 50 nm-thick film and was then annealed at 115°C for 10 min. The P3HT:ICBA solution was then statically dispensed with a micropipette onto the ITO coated boro-aluminosilicate glass substrate (Delta Technologies) and spin-coated at 900 RPM and 1450 RPM to deposit approximately 90 nm and 67 nm-thick films, respectively. The P3HT:ICBA thin films were baked at 70 °C for 5 minutes to remove any residual solvent. Afterwards, a 110 nm aluminum layer was deposited as a cathode in the e-beam evaporator, and then the devices were annealed at 150 °C for 15 min on a conventional hot plate. The active area of each device was about 0.9 cm^2.

Devices were illuminated with AM1.5 spectra of 50-60 mW/cm^2 optical power density from Spectra Physics 66900 solar simulator. The incident optical power density was measured with a Newport Oriel 91150V reference cell and meter. To control the temperature of the solar cells for testing, a thermoelectric Peltier module with a DC voltage supply, which uses voltage to change the temperature on the plates, was used. A non-contact infrared thermometer was also used to monitor the temperature. The I-V curves were measured for the temperature range from 20 °C to 65 °C using Keithley 2400 source meter. Fig. 1 (a$_1$) and (b$_1$) show experimentally obtained I-V curves under solar simulator illumination. From the I-V characteristics, the corresponding temperature-dependent I_{sc} and PCE were determined (Fig. 1 (a$_2$), (a$_3$), (b$_2$), and (b$_3$)).
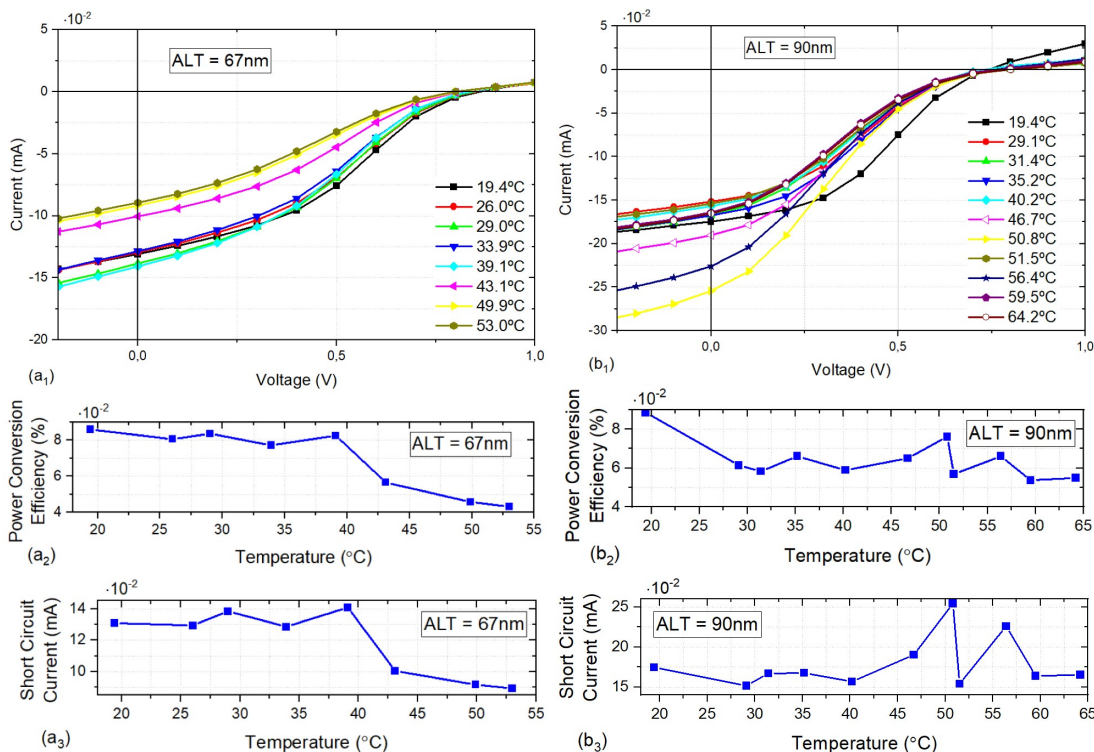

Fig. 1. Measured I-V characteristics of ITO/PEDOT:PSS/P3HT:ICBA/al solar cells with (a1) 67 nm and (b1) 90 nm active layer thicknesses at different Temperatures; (a2) and (b2) PCE and (a3) and (b3) Isc temperature dependencies for the same devices, respectively.

III. MODEL

To simulate the temperature dependence of ITO/PEDOT:PSS/P3HT:ICBA/Al solar cell characteristics, we used the DDM described in our previous research [32]. The Robin type boundary conditions which account for surface recombination on electrode contacts were applied [33]. Generation rate of charge carriers in the active layer was calculated using the transfer matrix method (TMM) which takes into account interference effects in the device [13]. The optical constants, refraction index, and extinction coefficient used in the TMM were determined from optical measurements that also take the interference effects in the thin organic films into account. As the transport mechanism of holes and electrons in polymer:fullerene blends are strongly thermally activated [14, 15], we supposed that temperature-dependent behaviour of ITO/PEDOT:PSS/P3HT:ICBA/Al solar cell is predominantly governed by temperature-dependent mobilities. Since mobility temperature dependence is much weaker for electrons than for holes [29], we assumed a constant electron mobility and an Arrhenius-type [15] temperature-dependent hole mobility:

$$\mu_p = \mu_{p0} e^{-\frac{\Delta}{k_b T}} \tag{1}$$

where μ_{p0} is a mobility prefactor, Δ is the activation energy, k_b Boltzmann's constant, and T the absolute temperature. The numerical DDM solution includes the Sharfetter-Gummel approach. All the other model methods and assumptions are the same as in [32].

IV. RESULTS AND DISCUSSION

The *I-V* characteristics for two ITO/PEDOT:PSS/P3HT:ICBA/Al devices with 67 nm and 90 nm thick P3HT:ICBA active layer measured at several different temperatures between 20 °C to 65 °C are shown in Fig. 1 a₁) and b₁). Both devices exhibit pronounced S-shape deformation. The deformation most likely originates from the aggravated extraction through the Al electrode and a consequent accumulation of the charge carriers. The PCE and I_{sc} as functions of T for two examined PSCs are presented in Fig. 1 a₂, a₃, b₂, and b₃. The non-mnotonic change of PCE and I_{sc} with temperature is apparent for both devices. While the PCE(T) had an overall decreasing character, the maximum of I_{sc} was obtained around 40 °C for the solar cell with 67 nm ALT and around 50 °C for the solar cell with 90 nm ALT. The tested devices had rather small PCE values due to inefficient cathode extraction.

The DDM simulations were conducted by using the parameter values given in Table 1. Because of the S-shape experimental *I-V* characteristics anomaly, it was proposed that surface recombination of electrons was pronounced at the cathode contact. The surface recombination velocities (SRVs) on the anode contact were taken to be infinite, while the electron SRV on the cathode was assumed to be reduced (Table 1). The calculated *I-V* curves for the 67 and 90nm ALT devices for the same T values at which the measurements were done are shown in Fig. 2 (a₁) and (b₁). The corresponding PCE(T) and $I_{sc}(T)$ were determined and depicted in Fig. 2 (a₂), (a₃), (b₂), and (b₃). From Fig. 2 (a₂) and (b₂) it can be noticed that theory predicts a slightly increasing trend for PCE(T). Also, the increasing trend for $I_{sc}(T)$ is obtained from calculations as can be seen from Fig. 2 (a₃) and (b₃). Since the experimental results given in Fig. 1 are qualitatively poorly reproduced by the model, a conclusion was drawn that the DDM which includes the effect of temperature on the PSC performance only through Arrhenius T-dependent hole transport is not adequate. Apparently, there are other processes that are significantly affected by T.

TABLE 1
THE PARAMETERS FOR ITO/PEDOT:PSS/P3HT:ICBA/AL SOLAR CELLS

Symbol	Quantity	Value
E_g	Energy gap	1.4eV
ε_r	Relative permittivity	3.4
N_C, N_V	The effective densities of states	$1 \times 10^{26} \text{m}^{-3}$
μ_{p0}	Hole mobility	$3 \text{ cm}^2/(\text{V·s})$
μ_n	Electron mobility	$4.92 \times 10^{-4} \text{ cm}^2/(\text{V·s})$
Δ	Activation energy	0.3eV
IQE	Internal quantum efficiency	0.05
τ_n	Electron lifetime	$6.2 \times 10^{-5} \text{s}$
τ_p	Hole lifetime	$3 \times 10^{-7} \text{s}$
S_n^c	Electron SRV at the cathode	$9.6 \times 10^{4} \text{cm/s}$

When a photon is absorbed in the PSC's active layer, the Coulombically bound electron-hole pair constituting an excitonic state is produced. It is known that temperature plays an important role in exciton dissociation [19, 34]. First, the charge transfer (CT) state is made at the donor/acceptor junction and some additional energy is needed to complete the dissociation. Thermal energy can be used for the separation of the CT state into free carriers [19, 34]. Knowing that the photogeneration in PSCs is affected by temperature, we attempted to reproduce the PSCs *I-V* characteristics at different T by letting the IQE be T-dependent and used it as a fitting parameter. The electron SRV on the cathode is also expected to change with T since it is essentially the Shockley-Read-Hall recombination through the surface trap states. For this reason, the SRV for electrons on the cathode was taken to be variable. When the IQE and electron SRV on the cathode were changed with T, a very good agreement between experimental and simulated *I-V* data was accomplished. The comparison of measured and DDM calculated *I-V* curves for solar cells with 67 nm and 90 nm ALTs for three selected temperatures is shown in Fig. 3. The built-in voltage was also slightly changed with temperature, which is denoted on each *I-V* graph. The IQE and SRV values at different T obtained for the two considered PSCs are presented in Table 2. The IQE changed with T in a nonmonotonic fashion, which was not the same for devices with different ALTs. This can be attributed to the P3HT:ICBA film morphology changes caused by the temperature and correlated to the film thickness [31]. On the other hand, the electron SRVs on the cathodes for both devices were decreasing with T, reflecting the fact that the surface (trap-assisted) recombination becomes more pronounced with increasing T.

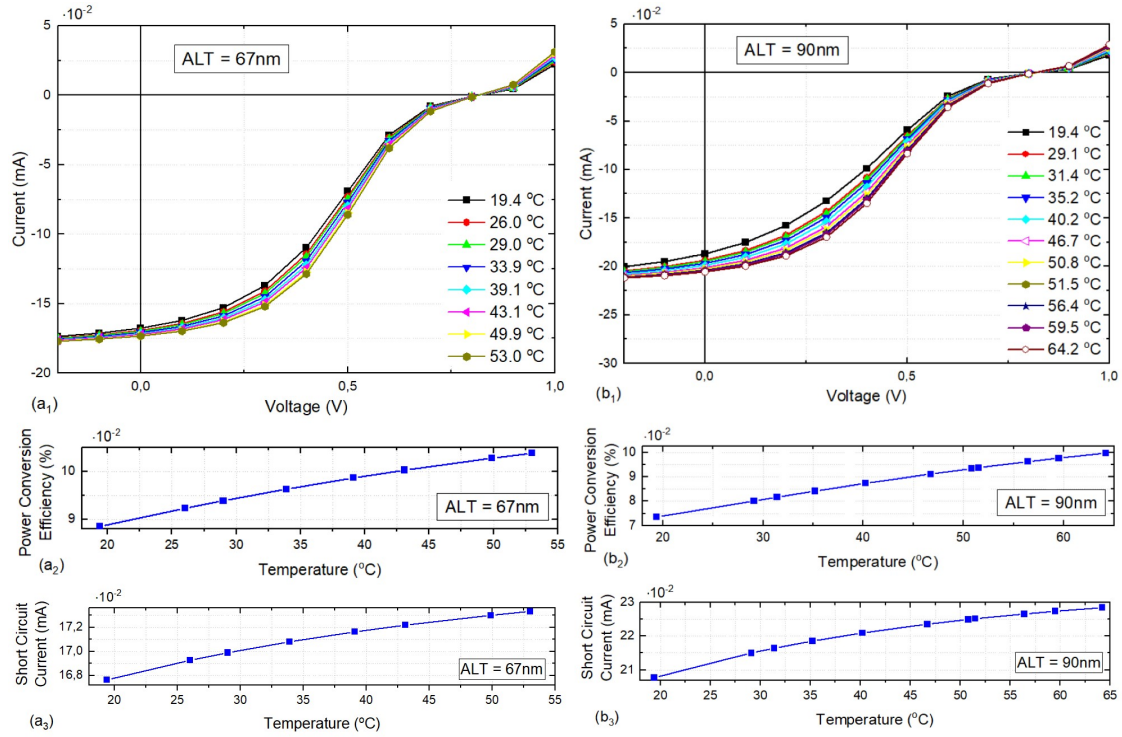Fig. 2. The I-V characteristics of ITO/PEDOT:PSS/P3HT:ICBA/al solar cells with (a1) 67 nm and (b1) 90 nm active layer thicknesses at different temperatures simulated by standard DDM including Arrhenius-type temperature-dependent hole mobility. The calculated (a2) and (b2) PCE and (a3) and (b3) Isc temperature-dependencies for the same devices, respectively.
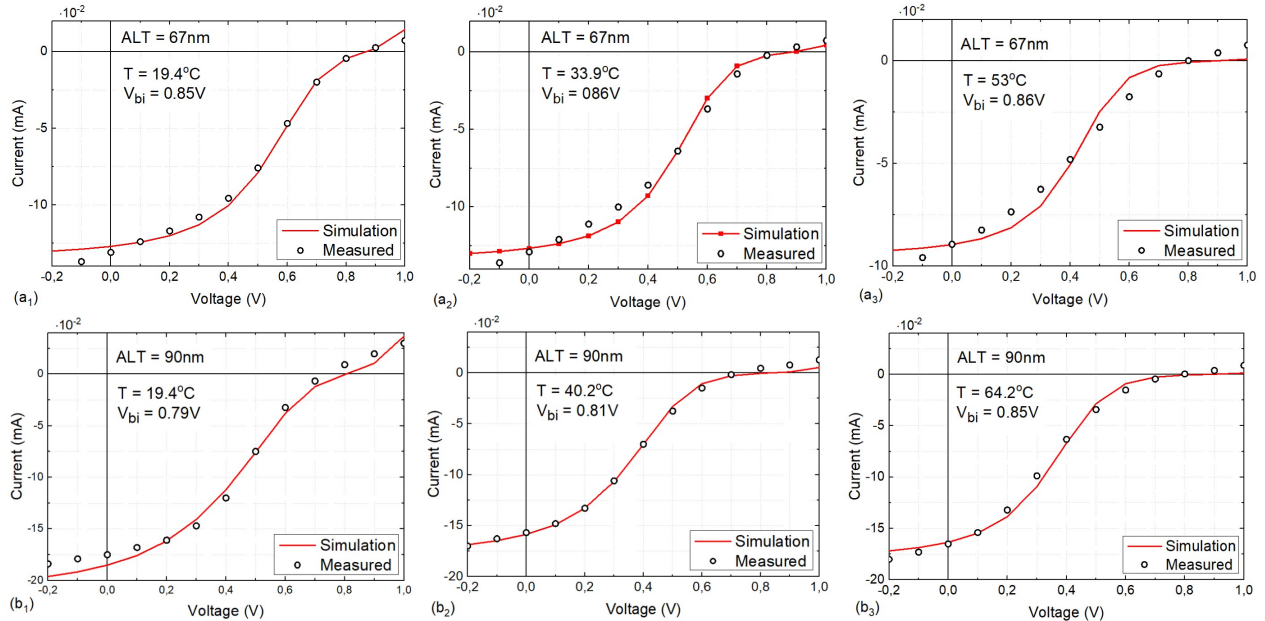

Fig. 3. Comparison of measured and simulated I-V characteristics of ITO/PEDOT:PSS/P3HT:ICBA/al solar cells with 67 nm and 90 nm active layer thicknesses at selected temperatures. Simulations are conducted using DDM with Arrhenius-type temperature-dependent hole mobility together with temperature-dependent IQE and electron SRV at the cathode.

V. CONCLUSION

Temperature influence on the performance of P3HT:ICBA solar cells was investigated. ITO/PEDOT:PSS/P3HT:ICBA/Al solar cells with two different ALTs were fabricated and characterized under solar simulator light. The I-V characteristics were measured within the temperature range of 20 °C-65 °C for both devices, and PCE and I_{sc} as functions of T were determined. The recorded I-V curves manifested the S-shape deviation. To simulate the I-V(T) data, the DDM model including surface recombination on both electrodes and Arrhenius-type T-dependent hole mobility was used and resulted in a poor agreement between theory and experiment. To better reproduce the experimental I-V curves, the T-dependent IQE and electron SRV at cathode were assumed and used in calculations as fitting parameters. This way, a very good

match of calculated with measured *I-V* curves was achieved in the whole temperature range. The obtained IQE(T) dependence was nonmonotonic and differed for solar cells with different ALTs. This was attributed to the temperature-induced morphology changes, which are strongly correlated with the P3HT:ICBA thin film thickness [31]. The electron SRV at the cathode showed increasing character with T, which is in accord with the fact that it is a trap-assisted recombination mechanism. A further study should be conducted to resolve the correlation between polymer thin film morphology, thickness, and applied temperature.

TABLE 2
THE IQE AND SRV VALUES AT DIFFERENT T

ALT= 90 nm		
T (°C)	IQE	Electron SRV [cm/s]
19.4	0.044	8.90×10^{-3}
29.1	0.037	4.55×10^{-4}
31.4	0.040	4.56×10^{-4}
35.2	0.040	5.74×10^{-5}
40.2	0.037	4.63×10^{-5}
46.7	0.046	4.68×10^{-5}
50.8	0.059	1.57×10^{-5}
51.5	0.036	1.57×10^{-5}
56.4	0.053	1.58×10^{-5}
59.5	0.037	4.77×10^{-6}
64.2	0.037	4.80×10^{-6}
ALT= 67 nm		
T (°C)	IQE	Electron SRV [cm/s]
19.4	0.037	4.47×10^{-3}
26.0	0.037	6.46×10^{-4}
29.0	0.040	3.03×10^{-4}
33.9	0.037	1.99×10^{-4}
39.1	0.040	9.24×10^{-5}
43.1	0.029	4.65×10^{-5}
49.9	0.027	2.35×10^{-5}
53.0	0.026	6.75×10^{-6}

REFERENCES

[1] M. B. Salim, R. Nekovei, and R. Jeyakumar, "Organic tandem solar cells with 18.6% efficiency," *Solar Energy*, vol. 198, pp. 160–166, Mar. 2020, doi: 10.1016/j.solener.2020.01.042.

[2] Q. Liu, Y. Jiang, K. Jin, J. Qin, J. Xu, W. Li, J. Xiong, J. Liu, Z. Xiao, K. Sun, S. Yang, X. Zhang, and L. Ding, "18% Efficiency organic solar cells," *Science Bulletin*, vol. 65, no. 4, pp. 272–275, Feb. 2020, doi: 10.1016/j.scib.2020.01.001.

[3] H. Chen, J. Hou, S. Zhang, Y. Liang, G. Yang, Y. Yang, L. Yu, Y. Wu and G. Li, "Polymer solar cells with enhanced open-circuit voltage and efficiency," *Nature Photon*, vol. 3, no. 11, pp. 649–653, Nov. 2009, doi: 10.1038/nphoton.2009.192.

[4] K. Kawashima, Y. Tamai, H. Ohkita, I. Osaka, and K. Takimiya, "High-efficiency polymer solar cells with small photon energy loss," *Nat Commun*, vol. 6, no. 1, p. 10085, Dec. 2015, doi: 10.1038/ncomms10085.

[5] H. Kang, W. Lee, J. Oh, T. Kim, C. Lee, and B. J. Kim, "From Fullerene–Polymer to All-Polymer Solar Cells: The Importance of Molecular Packing, Orientation, and Morphology Control," *Acc. Chem. Res.*, vol. 49, no. 11, pp. 2424–2434, Nov. 2016, doi: 10.1021/acs.accounts.6b00347.

[6] S. Jin, B. V. K. Naidu, H. Jeon, S. Park, J. Park, S. C. Kim, J. W. Lee, Y. Gal, "Optimization of process parameters for high-efficiency polymer photovoltaic devices based on P3HT:PCBM system," *Solar Energy Materials and Solar Cells*, vol. 91, no. 13, pp. 1187–1193, Aug. 2007, doi: 10.1016/j.solmat.2007.04.001.

[7] J. G. Sanchez, A. A. A. Torimtubun, V. S. Balderrama, M. Estrada, J. Pallares, and L. F. Marsal, "Effects of Annealing Temperature on the Performance of Organic Solar Cells Based on Polymer: Non-Fullerene Using V$_2$O$_5$ as HTL," *IEEE J. Electron Devices Soc.*, vol. 8, pp. 421–428, 2020, doi: 10.1109/JEDS.2020.2964634.

[8] Y. Liu, J. Zhao, Z. Li, C. Mu, W. Ma, H. Hu, K. Jiang, H. Lin, H. Ade, and H. Yan, "Aggregation and morphology control enables multiple cases of high-efficiency polymer solar cells," *Nat Commun*, vol. 5, no. 1, p. 5293, Dec. 2014, doi: 10.1038/ncomms6293.

[9] F. Cheng, G. Fang, X. Fan, H. Huang, Q. Zheng, P. Qin, H. Lei, and Y. Li, "Enhancing the performance of P3HT:ICBA based polymer solar cells using LiF as electron collecting buffer layer and UV–ozone treated MoO3 as hole collecting buffer layer," *Solar Energy Materials and Solar Cells*, vol. 110, pp. 63–68, Mar. 2013, doi: 10.1016/j.solmat.2012.12.006.

[10] S. B. Jo, Y. Liu, F. Lin, and A. K. -Y. Jen, "Tackling Energy Loss for High-Efficiency Organic Solar Cells with Integrated Multiple Strategies," *Adv. Mater.*, vol. 30, no. 16, p. 1706816, Apr. 2018, doi: 10.1002/adma.201706816.

[11] W. Cai, X. Gong, and Y. Cao, "Polymer solar cells: Recent development and possible routes for improvement in the performance," *Solar Energy Materials and Solar Cells*, vol. 94, no. 2, pp. 114–127, Feb. 2010, doi: 10.1016/j.solmat.2009.10.005.

[12] L. J. A. Koster, E. C. P. Smits, V. D. Mihailetchi, and P. W. M. Blom, "Device model for the operation of polymer/fullerene bulk heterojunction solar cells," *Phys. Rev. B*, vol. 72, no. 8, p. 085205, Aug. 2005, doi: 10.1103/PhysRevB.72.085205.

[13] L. A. A. Pettersson, L. S. Roman, and O. Inganäs, "Modeling photocurrent action spectra of photovoltaic devices based on organic thin films," *Journal of Applied Physics*, vol. 86, no. 1, pp. 487–496, Jul. 1999, doi: 10.1063/1.370757.

[14] V. D. Mihailetchi, H. X. Xie, B. de Boer, L. J. A. Koster, and P. W. M. Blom, "Charge Transport and Photocurrent Generation in Poly(3-hexylthiophene): Methanofullerene Bulk-Heterojunction Solar Cells," *Adv. Funct. Mater.*, vol. 16, no. 5, pp. 699–708, Mar. 2006, doi: 10.1002/adfm.200500420.

[15] F. Laquai, D. Andrienko, R. Mauer, and P. W. M. Blom, "Charge Carrier Transport and Photogeneration in P3HT:PCBM Photovoltaic Blends," *Macromol. Rapid Commun.*, vol. 36, no. 11, pp. 1001–1025, Jun. 2015, doi: 10.1002/marc.201500047.

[16] Y. Min Nam, J. Huh, and W. H. Jo, "A computational study on optimal design for organic tandem solar cells," *Solar Energy Materials and Solar Cells*, vol. 95, no. 4, pp. 1095–1101, Apr. 2011, doi: 10.1016/j.solmat.2010.12.018.

[17] A. Cheknane, H. S. Hilal, F. Djeffal, B. Benyoucef, and J.-P. Charles, "An equivalent circuit approach to organic solar cell modelling," *Microelectronics Journal*, vol. 39, no. 10, pp. 1173–1180, Oct. 2008, doi: 10.1016/j.mejo.2008.01.053.

[18] G. Li, L. Liu, F. Wei, S. Xia, and X. Qian, "Recent Progress in Modeling, Simulation, and Optimization of Polymer Solar Cells," IEEE J. Photovoltaics, vol. 2, no. 3, pp. 320–340, Jul. 2012, doi: 10.1109/JPHOTOV.2012.2193385.

[19] C. Ma, C. C. S. Chan, X. Zou, H. Yu, J. Zhang, H. Yan, K. S. Wong, and P. C. Y. Chow, "Unraveling the Temperature Dependence of Exciton Dissociation and Free Charge Generation in Nonfullerene Organic Solar Cells," *Sol. RRL*, vol. 5, no. 4, p. 2000789, Apr. 2021, doi: 10.1002/solr.202000789.

[20] A. Mahmoudloo and S. Ahmadi-Kandjani, "Influence of the temperature on the charge transport and recombination profile in organic bulk heterojunction solar cells: a drift-diffusion study," *Appl. Phys. A*, vol. 119, no. 4, pp. 1523–1529, Jun. 2015, doi: 10.1007/s00339-015-9130-3.

[21] K. Tvingstedt, J. Benduhn, and K. Vandewal, "Temperature dependence of the spectral line-width of charge-transfer state emission in organic solar cells; static *vs.* dynamic disorder," *Mater. Horiz.*, vol. 7, no. 7, pp. 1888–1900, 2020, doi: 10.1039/D0MH00385A.

[22] S. A. Hawks, G. Li, Y. Yang, and R. A. Street, "Band tail recombination in polymer:fullerene organic solar cells," *Journal of Applied Physics*, vol. 116, no. 7, p. 074503, Aug. 2014, doi: 10.1063/1.4892869.

[23] S. R. Cowan, N. Banerji, W. L. Leong, and A. J. Heeger, "Charge Formation, Recombination, and Sweep-Out Dynamics in Organic Solar Cells," *Adv. Funct. Mater.*, vol. 22, no. 6, pp. 1116–1128, Mar. 2012, doi: 10.1002/adfm.201101632.

[24] S. R. Cowan, A. Roy, and A. J. Heeger, "Recombination in polymer-fullerene bulk heterojunction solar cells," *Phys. Rev. B*, vol. 82, no. 24, p. 245207, Dec. 2010, doi: 10.1103/PhysRevB.82.245207.

[25] A. Petrovic, J. Gojanovic, P. Matavulj, M. Islam, and S. Zivanovic, "Temperature dependence of P3HT:ICBA polymer solar cells," in *2017 International Conference on Numerical Simulation of Optoelectronic Devices (NUSOD)*, Copenhagen, Denmark, Jul. 2017, pp. 133–134. doi: 10.1109/NUSOD.2017.8010027.

[26] G. Garcia-Belmonte, "Temperature dependence of open-circuit voltage in organic solar cells from generation–recombination kinetic balance," *Solar Energy Materials and Solar Cells*, vol. 94, no. 12, pp. 2166–2169, Dec. 2010, doi: 10.1016/j.solmat.2010.07.006.

[27] I. Riedel, J. Parisi, V. Dyakonov, L. Lutsen, D. Vanderzande, and J. C. Hummelen, "Effect of Temperature and Illumination on the Electrical Characteristics of Polymer–Fullerene Bulk-Heterojunction Solar Cells," *Adv. Funct. Mater.*, vol. 14, no. 1, pp. 38–44, Jan. 2004, doi: 10.1002/adfm.200304399.

[28] K. Tvingstedt and C. Deibel, "Temperature Dependence of Ideality Factors in Organic Solar Cells and the Relation to Radiative Efficiency," *Adv. Energy Mater.*, vol. 6, no. 9, p. 1502230, May 2016, doi: 10.1002/aenm.201502230.

[29] B. Yang, J. Cox, Y. Yuan, F. Guo, and J. Huang, "Increased efficiency of low band gap polymer solar cells at elevated temperature and its origins," *Appl. Phys. Lett.*, vol. 99, no. 13, p. 133302, Sep. 2011, doi: 10.1063/1.3643450.

[30] W. Bagienski and M. C. Gupta, "Temperature dependence of polymer/fullerene organic solar cells," *Solar Energy Materials and Solar Cells*, vol. 95, no. 3, pp. 933–941, Mar. 2011, doi: 10.1016/j.solmat.2010.11.026.

[31] J. Vlahović, M. Stanojević, J. Gojanović, J. Melancon, A. Sharma, and S. Živanović, "Thickness dependent photocurrent spectra and current-voltage characteristics of P3HT:PCBM photovoltaic devices," *Opt. Express*, vol. 29, no. 6, p. 8710, Mar. 2021, doi: 10.1364/OE.418082.

[32] Ž. Jelić, J. Petrović, P. Matavulj, J. Melancon, A. Sharma, C. Zellhofer, and S. Živanović, "Modeling of the polymer solar cell with a P3HT:PCBM active layer," Phys. Scr., vol. T162, p. 014035, Sep. 2014, doi: 10.1088/0031-8949/2014/T162/014035.

[33] A. R. Khalf, J. P. Gojanovic, N. A. Cirovic, S. Zivanovic, and P. S. Matavulj, "The Impact of Surface Processes on the J–V Characteristics of Organic Solar Cells," *IEEE J. Photovoltaics*, vol. 10, no. 2, pp. 514–521, Mar. 2020, doi: 10.1109/JPHOTOV.2020.2965401.

[34] S. Ono and K. Ohno, "Origin of Charge Transfer Exciton Dissociation in Organic Solar Cells," in *Excitons*, S. L. Pyshkin, Ed. InTech, 2018. doi: 10.5772/intechopen.69854.